Macromolecules
ARTICLE

Macromolecules **2010**, *43*, 9957–9963 **9957**
DOI: 10.1021/ma101511p

Controlled Poly(ethylene glycol) Network Structures through Silsesquioxane Cross-Links Formed by Sol−Gel Reactions

Babak Radi, R. Mark Wellard, and Graeme A. George*

Institute of Health and Biomedical Innovation and Chemistry Discipline, Faculty of Science and Technology Queensland University of Technology, Brisbane 4000, Australia

Received July 6, 2010; Revised Manuscript Received October 7, 2010

ABSTRACT: A new type of poly(ethylene glycol) [PEG] hydrogel network was synthesized that is cross-linked through silsesquioxane domains [$SiO_{1.5}$] formed by hydrolysis and condensation of a bis(triethoxy silyl propyl urethane)−PEG-2000 precursor. Step crystallization−DSC and DMTA techniques were used to characterize the PEG domains in the dry network while silsesquioxane cross-link structures and connectivity were determined by ^{29}Si solid state NMR. No evidence was found by ^{29}Si NMR or TEM for the formation of silica domains [SiO_2]. The concentration of added acid in the sol−gel reaction controls the kinetics of the silsesquioxane formation and thus the size of these domains. Water-swelling studies confirm that when the particles are formed slowly (at lower acid concentration) there is an increase in the cross-link density and connectivity; i.e. the number of chains attached to each silsesquioxane domain. High connectivity also reduces the crystallinity of PEG in the dry network and results in a shift in both α- and α′-transitions to lower temperatures.

Introduction

Since Wichterle and Lim in 1960 worked on cross-linked hydroxyethyl methacrylate (HEMA),[1] hydrogels and gels have been of interest in biomedical applications such as tissue engineering, implant materials and drug delivery systems.[2−4] Poly(ethylene glycol) [PEG] networks, copolymers and hydrogels have had a special role in these and related applications in wound healing and cell migration[5,6] because the hydrophilic and biocompatible PEG chain resists protein absorption.[7]

The mesh size also controls the percentage of swelling of the network at equilibrium as well as acting as a size exclusion agent for macromolecular sorbates such as proteins.[8−10] The mesh size is able to be tailored by: the average molecular weight between cross-links, M_c, the initial monomer or precursor (macromonomer) concentration,[11] porogens introduced during hydrogel synthesis,[12,13] and the type and functionality of the cross-link structure. In principle the mesh size increases with a larger M_c while the precursor concentration elicits the opposite effect. The concentration increase causes an increase in the number of permanent entanglements between two cross-link junctions. The permanent entanglements effectively decrease M_c as described by Hennink et al.,[11] so as a result the mesh size becomes smaller.

The network that is synthesized from a multi functional polymer precursor (macromonomer) produces a variety of cross-link structures when the cross-linking reaction is a controllable process. Currently reported methods of PEG network synthesis involve different precursors such as double-bond terminated PEG for free radical reaction;[5] multi arm PEG terminated with amino groups that react through Michael addition to give bridging groups having matrix metalloproteinase- (MMP) or plasmin-sensitive peptide sequences;[7] urethane linkages from reaction of a trifunctional isocyanate with terminal hydroxyl groups of PEG and bis(triethoxy silyl propyl urethane)−PEG-2000 which reacts with tetraethyl orthosilicate (TEOS) to form a hybrid organic−inorganic network.[14,15] All of these approaches have some limitations. For example, it is known that the PEG−urethane network can be synthesized with different cross-link structures and mesh size by changing the ratio between isocyanate and PEG.[16] However, when the molar ratio of the NCO group to the OH group is lower than the stoichiometric value, dangling chains result which can change network properties such as swelling.

We have developed a method to form PEG networks using sol−gel chemistry which is novel for hydrogel synthesis with controlled structure by using a silsesquioxane cross-linker formed from a multifunctional silane in the *absence* of TEOS. Silsesquioxane cross-link structures are tailored via sol−gel reaction conditions such as pH and amount of added water without leaving dangling chains. The silsesquioxane structures can be altered by the rate of hydrolysis and condensation reactions.[17] In particular, the cross-linking and chain extension reactions are sensitive to pH. From studies on TEOS silica precursors, at low pH, linear chain extension with a low degree of cross-linking occurs, whereas at higher pH the dominant process is a highly branched and cross-linking polymerization.[18,19] As a result, it would be expected that at low pH small size silsesquioxane domains would be formed and at higher pH larger silsesquioxane domains should be seen.

This silsesquioxane structural control strategy has been employed to tailor PEG network structures and properties in this research.

Experimental Section

Materials. Poly(ethylene glycol) (PEG, MW = 2000) was purchased from Sigma −Aldrich. It was dried by azeotropic distillation with toluene under an ultra high purity argon blanket. 3-(Triethoxysilyl)propyl isocyanate (95%) and 1,4-diazabicyclo-[2.2.2]octane (triethylenediamine) (99%) were purchased from Sigma-Aldrich. Toluene (HPLC grade) was purchased from Burdick & Jackson and hydrochloric acid (32%) was purchased from Univar as analytical grade. The deionized water was purified by a USF Elga (Maxima SC) deionizer system.

*Corresponding author. E-mail: g.george@qut.edu.au.

Published on Web 11/03/2010

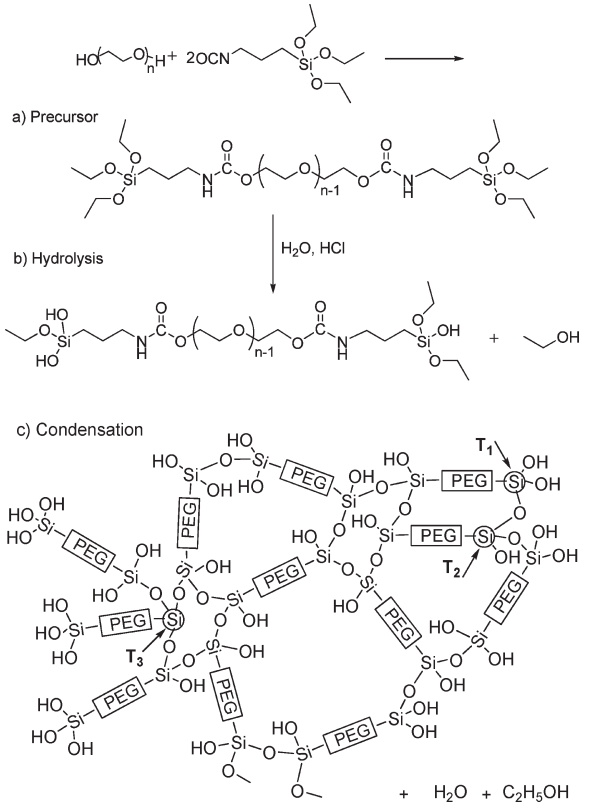

Figure 1. Reaction sequence for the synthesis of (a) the precursor (bis(triethoxy silyl propyl urethane)−PEG-2000) and (b) the hydrolysis and (c) condensation reactions for formation of the silsesquioxane cross-linked PEG network. Note the boxed [PEG] symbol represents a diurethane−PEG structure linking to the hydrolyzed and condensed silane groups. One example of each type of silsesquioxane junction formed (T_1, T_2, T_3 in Figure 4) is also shown.

Synthesis of Bis(triethoxy silyl propyl urethane)−PEG-2000. The reaction sequence is shown in Figure 1 (a). The dry PEG of M_n = 2000 g/mol (5 g, 2.5 mmol) was dissolved in 125 mL of toluene and a 20% molar excess (based on hydroxyl group concentration in PEG) of 3-(triethoxysilyl)propyl isocyanate (1.5 mL, 6 mmol) was added under argon flow together with triethylenediamine (100 mg) as catalyst.[20] The solution was stirred for 40 h under argon at 85 °C. Solvent was removed by rotary evaporator and high vacuum followed by sublimation of any remaining catalyst. Fourier transform infrared (FT-IR), ^{13}C NMR, ^{1}H NMR, 2D proton-carbon HSQC NMR, and ^{29}Si NMR spectra were collected of the reaction product which was then sealed and stored under argon.

Synthesis of Silsesquioxane Cross-Linked PEG Network in Solution with Different Amounts of Hydrochloric Acid. The reaction sequence is shown in Figure 1, parts b and c. Four different series of networks were synthesized with different amounts of 0.1 M hydrochloric acid solution as a sol−gel chemistry reaction. Bis(triethoxy silyl propyl urethane)−PEG-2000 (precursor) (0.25 g) was dissolved in methanol (0.15 g, 0.19 mL) in polypropylene sample tubes with caps. After agitation in the ultrasonic bath for 5 min, the sample tubes were heated, open, in an oven at 50 °C for about 6 h to evaporate the methanol. Deionized water (0.15 mL, 8.3 mmol) was added to all sample tubes; the caps were tightened and kept at 38 °C overnight under saturated humidity conditions. A different amount of hydrochloric acid solution (0.1 M) was added to each sample tube (SW1, 0.05 mL; SW2, 0.10 mL; SW3, 0.150 mL; SW4, 0.200 mL). The calculated concentration of acid for each addition is given in Table 1. The solutions were extensively shaken to synthesize homogeneous networks. The capped sample tubes were held overnight at 45 °C and 24 h at 50 °C for further reaction under saturated humidity conditions,

Table 1. Crystal Transition Temperature (T_m) and the Enthalpy of Fusion (ΔH_f) in PEG 2000 and PEG−Silsesquioxane Networks Synthesized with [H_3O^+]

network	[H_3O^+] (mol/L)	T_m (°C)	ΔH_f (J/g)
SW 1	0.011	21.8	47.93
SW 2	0.020	28.4	59.46
SW 3	0.0273	29.8	61.53
SW 4	0.0333	30.8	62.72
PEG 2000		52.9	183.4

samples were dried by removing the sample tube caps in the oven at 50 °C for 6 h, and then held under vacuum at 60 °C for around 48 h to postcure. ^{29}Si solid-state CP/MAS NMR spectroscopy was used to determine the nature of the silsesquioxane structures (T_0, T_1, T_2, and T_3) in the dry networks that were synthesized under different conditions of acid addition. Figure 1c shows the different possible structures that may form from the condensation reactions.

Swelling Studies. The mass of the completely dry networks was recorded at room temperature (w_{id}). The samples were immersed in deionized water, which was changed every day, to remove all starting materials and un-cross-linked polymers. The surface of the hydrogel was dried with a filter paper, and the mass of the swollen hydrogel was recorded (w_{sw}). This was repeated until the sample reached constant weight (ie. was at equilibrium). The hydrogels were partially dried at room temperature, and then held under vacuum at 40 °C for at least 4 days. The mass of the dry samples was recorded (w_d). These dry networks and swollen hydrogel mass data were used to calculate the sol fraction and swelling percentage at equilibrium.

$$\text{swelling } \% = \frac{w_{sw} - w_d}{w_d} \times 100 \quad (1)$$

$$\text{sol } \% = \frac{w_{id} - w_d}{w_d} \times 100 \quad (2)$$

Step Crystallization Differential Scanning Calorimetry (SC−DSC). Small quantities of the dry networks (2−4 mg) were sealed in aluminum DSC pans for analysis on a TA Instrument DSC Q100 under a flow of 40 mL/min of nitrogen. In running step crystallization DSC,[21] the samples were equilibrated at 100 °C for 5 min, then rapidly cooled to 60 °C and equilibrated for 30 min at this temperature. In subsequent steps the temperature decreased by 4 °C and the samples were kept in an isothermal condition for 30 min. The cooling process ended at −30 °C. The samples were equilibrated at −80 °C and were then heated to 100 at 5 °C/min.

Dynamic Mechanical Thermal Analysis (DMTA). Disk-shape samples (7 mm diameter x 3 mm) were run on a Mettler Toledo DMA/SDTA861e instrument. The experiments were run in compression mode at 5 Hz from −90 to +50 °C with a temperature ramp 2 °C/min. The settings for each dry sample were obtained with an isothermal-strain sweep run at 25 °C.

FT-IR Spectra. ATR-IR spectra of polymer products were obtained using a diamond ATR cell on a Nicolet Nexus 870 spectrometer

^{13}C NMR, ^{1}H NMR, and 2D Proton−Carbon HSQC NMR. The spectra of products were recorded on Varian 400 direct drive NMR spectrometer using a 5 mm AUTOX probe. The samples were dissolved in chloroform-d_1 at a concentration of 50 mg per 1 mL. NMR tubes were treated with Sigmacote to remove all Si−OH groups.

^{29}Si Solid State CP/MAS NMR. ^{1}H decoupled solid-state ^{29}Si cross polarized (CP)/magic angle spinning (MAS) NMR spectra were recorded on a Varian 400-MR NMR spectrometer with a 5 mm cpmas probe, operating at 79.43 MHz for silicon. Spectra, referenced to tetramethylsilane (TMS), were recorded with the tancpx pulse sequence in a 5 mm silicon nitride rotor spinning at

3.5 kHz. Spinal decoupling was used with a contact time of 3 ms. A sample temperature of 298 K was used and 25000 transients were recorded with 2000 data points over a spectral width of 500 ppm using a recycle time of 1 s and an acquisition time of 0.0495 s. Spectra were processed with the standard spectrometer software and peaks were fitted using MestReC software.

Thermogravimetric Analysis (TGA). To measure the percentage of silsesquioxane groups in the PEG networks, small quantities of the dry networks (10 mg) were put in a platinum pan for analysis on a TA Instrument (TGA Q500) under a flow of nitrogen up to 450 at 5 °C/min heating rate and then under oxygen up to 1000 °C at the same rate.

Transmission Electron Microscopy (TEM). To see possible nano structure of the PEG networks, the dry samples were rapidly frozen in liquid nitrogen and ultrathin sections (approximately 80 nm) were cut on a Leica Em UC6-Ultramicrotome. The TEM images were collected on a Philips CM200 microscope operating at 160 kV.

Results and Discussion

Synthesis of Networks. Sol−gel chemistry was employed as the cross-linking reaction method and to control the mesh size of the network. In the first step, the precursor was synthesized through reaction between hydroxyl groups at the ends of PEG chain and isocyanate groups in 3-(triethoxysilyl)propyl isocyanate in the presence of triethylenediamine as a catalyst at 85 °C in dry conditions (Figure 1). After evaporation of solvent and further purification under vacuum the structure of the precursor was characterized by:

- FT-IR by the total consumption of the isocyanate (disappearance of band at 2270 cm^{-1}) and the presence of a urethane linkage (C═O stretching and −NH bend of urethane, at 1740 to 1700 cm^{-1} and around 1530 cm^{-1}, respectively[22]) (Figure SI 1, Supporting Information)
- ^{1}H NMR demonstration conversion of starting material to precursor by appearance of signals at 4.15 ppm ($OCH_2C\boldsymbol{H_2}OCONH$) and at 4.98 ppm ($OCH_2CH_2OCO\boldsymbol{NH}$) (Figure SI 3, Supporting Information). The ^{1}H NMR spectrum in bis(triethoxy silyl propyl urethane)−PEG-2000 has several overlapping peaks so ^{13}CNMR and 2D NMR are required for full elucidation.
- ^{13}C NMR demonstrating conversion of starting material to precursor by the disappearance of signals at 72.5 ppm (OCH_2CH_2OH) and 61.5 ppm (OCH_2CH_2OH) and appearance of signals at 156.2 ppm (C═O in the urethane bond), at 69.5 ppm (OCH_2CH_2OCONH) and 63.6 ppm (OCH_2CH_2OCONH). (Figures SI 2, SI 3 and SI 4, Supporting Information) Assignments were confirmed with 2D proton−carbon HSQC (Figure SI 5, Supporting Information).
- ^{29}Si solid state MAS NMR by the presence of a band at −46 ppm attributed to the bis(triethoxy silyl) terminal group (Figure SI 6, Supporting Information).

As detailed in the Experimental Section, the silane in the precursor was transformed to a cross-link site[14,15] by the addition of acid to promote hydrolysis and condensation and as discussed later the sol−gel reaction conditions have been found to control the type and size of the silsesquioxane (Figure 1c). The percentage of silsesquioxane cross-linker was measured by TGA to be 6.25 wt %, present as SiO_2 structures in the dry network after burning in oxygen (Figure SI 7, Supporting Information).[23] Since the silicon is present in the original network as an organo-linked structure then calculating the content on a silsesquioxane composition of [$SiO_{1.5}$], the value is 5.4%. This compares with a theoretical content of 5.5 wt % from the original components.

Scheme 1. Mechanism of Hydrolysis and Condensation Reactions in an Acid-Catalyzed Sol−Gel Reaction of a Trialkoxy Silane[18] To Form Silsesquioxane Cross-Links

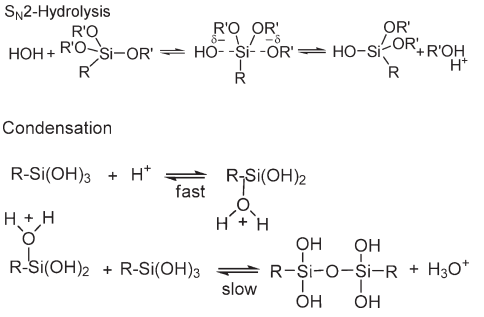

In this sol−gel process, alkoxide groups in precursor are partially or completely replaced by hydroxyl groups during the hydrolysis reaction. Aelion et al.[24] found the rate and extent of the hydrolysis reaction to be influenced by the presence of strong acid or base as a catalyst. Hydrolysis takes place by the nucleophilic attack (S_N2) of the oxygen in the water molecule on the silicon atom in precursor.[25] The rate of hydrolysis is first order in both acid and water concentration.[24]

The subsequent condensation reaction occurs from either fully (water-producing) or partially (alcohol-producing) hydrolysis reaction products.[18,26] The rate of condensation is first-order in acid and second-order in silanetriol:

$$R = k[\mathrm{RSi(OH)_3}]^2[\mathrm{H^+}] \quad (3)$$

Voronkov et al.[27] have reported that the rate of condensation increases with an increase in the number of silanols (hydrolyzed groups) on the silicon atom. According to Osterholz and Pohl,[25] the rate of condensation reaction in silsesquioxane formation depends on the electron donor which is covalently bonded to silicon. In the presence of a stronger electron donor the minimum rate of condensation shifts to lower pH. Scheme 1 shows the mechanism of the silsesquioxane cross-linking.

By analogy, the silsesquioxane structures can be controlled by the pH dependence of the rate of hydrolysis and condensation reactions.[17] In particular the pH should affect the connectivity of the silsesquioxane cross-linking domains by controlling their size.

Characterization of Networks. Techniques used to characterize the networks formed under different conditions of sol−gel synthesis include step crystallization-differential scanning calorimetry (SC-DSC) to probe the crystalline regions and dynamic mechanical thermal analysis (DMTA) which probes both amorphous and crystalline regions. When swollen with water, the silsesquioxane cross-linked network structure is expected to be totally amorphous and no crystallinity may be detected. However in a dried network the PEG chains of M_n = 2000 g/mol, in spite of being cross-linked, are able to pack to form crystalline regions. The crystallization process differs from normal crystallization of PEG since the chains are constrained by the silsesquioxane to which they are chemically bonded. As a result, the ultimate crystalline structures in the dry PEG network are altered by the sol−gel reaction conditions compared to the un-cross-linked PEG (Figure 2).

In SC−DSC, the shifts in crystal transition temperature result from the structural changes in the network[21] with the most stable crystalline structure showing the highest crystal transition temperature. In Figure 2, the lowest crystal transition temperature appeared in the network that was synthesized with the lowest amount of 0.1 M HCl solution (SW1) and the

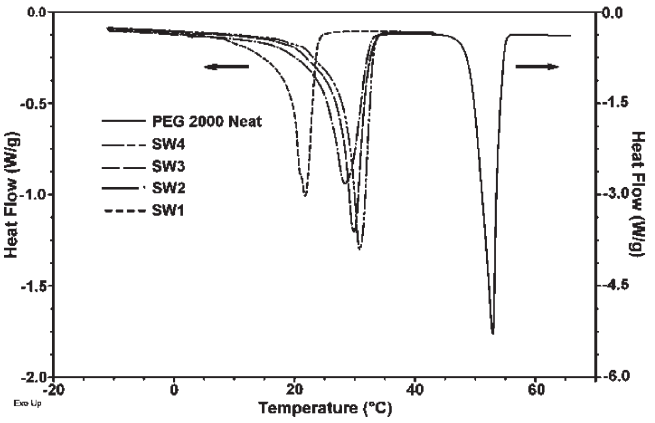

Figure 2. SC−DSC of dry PEG 2000 and PEG−silsesquioxane networks showing the shift in crystal transition temperature with the increasing size of silsesquioxane domains from SW4 to SW1.

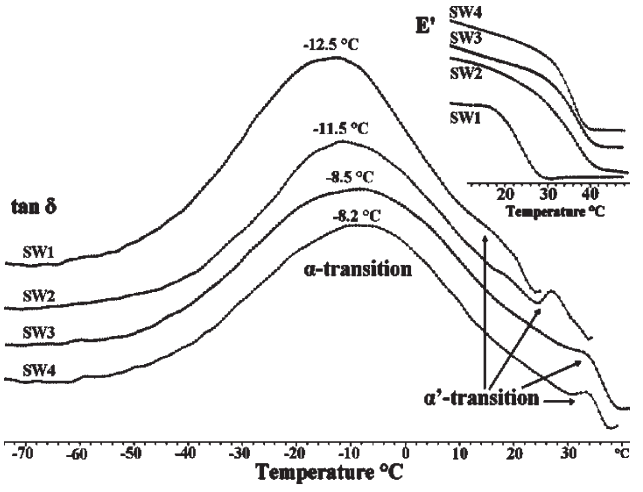

Figure 3. DMTA results for E′ and tan δ (both the α- and α′-transition) show differences between the PEG networks. The α-transition (T_g) shifts to higher temperature from SW1 to SW4. The α′-transition also moves to higher temperature. The E′ value decrease on crystal melting shows the same trend as that seen for both the α- and α′-transition. (Note that the curves have been offset vertically for clarity and absolute values of tan δ and E′ are not shown.)

highest temperature (except in neat PEG 2000) was seen in the network that was synthesized with the highest amount of 0.1 M HCl solution (SW4), but the shift is nonlinear with concentration. As shown in Figure 2, PEG 2000 has a melting point (T_m) ~30 °C higher than the cross-linked samples. This suggests the silsesquioxane cross-links hinder the crystallization process due to both an increase in the chain irregularity and reduced chain flexibility, which are necessary in the packing process. In Table 1 the crystalline transition temperatures in the networks and T_m of PEG 2000 are shown. The enthalpy of fusion (ΔH_f) shows that the degree of crystallinity undergoes a big decrease from PEG 2000 to all of the silsesquioxane -cross-linked networks. This decrease is greater the higher the pH (less amount of acidified water added), reflecting the progressive increase in the size of the silsesquioxane domains from SW4 to SW1.

From the photographs of the gels (Figure SI 8, Supporting Information) the change in the size of the PEG crystalline regions may be seen qualitatively by the increased opacity of the samples. Note that since the silsesquioxane cannot be resolved by TEM (Figure SI 9, Supporting Information) and the amount is only 5.5 wt %, it is impossible for light to be scattered by the silsesquioxane domains. Uniform concentration of elemental silicon was seen by energy-dispersive X-ray analysis (EDS) in the TEM, and no electron diffraction could be seen. The SW1 network is the most transparent sample at room temperature (around 23 °C) because it is above the crystal transition temperature of PEG (see Figure 2) and is not scattering light. The SW2 network is partially opaque, and the two other samples with a higher amount of 0.1 M HCl solution are totally opaque. The results in Figure 2 and the photographs in Figure SI 8, Supporting Information, show that the crystalline domains can be altered by the amount of added 0.1 M HCl solution, but other techniques are required to more precisely define the physical changes occurring.

DMTA results in Figure 3 show that the α-transition temperature, α′-transition temperature, and storage modulus (E′) versus temperature also underwent shifts with an increasing amount of acidic water used in synthesis from network SW1 to network SW4. The α′-transition that appears in some semicrystalline polymers, such as PEG, is an extra relaxation peak between the glass transition temperature and melting point. This can be distinguished from the crystalline transition by the frequency dependence of the α′-transition.[28,29] The α′-transition is sensitive to the crystalline structure developed by the dry network since it is caused by the flip-flop mechanism and/or the screw motion of the backbone atoms of the polymer in the crystal lattice.[28−30]

The α′-transition temperature and intensity depend on the crystalline regions' size, structures, and number of defects either on or inside the crystalline regions. From Figure 3, it is seen that the α′-transition occurred at the lowest temperature in sample SW1, and with an increasing amount of 0.1 M HCl solution it shifted to higher temperature. The storage modulus, E' versus temperature curve in a semicrystalline polymer shows a decrease in the rubbery region very close to polymer melting point in thermoplastics. In Figure 3, E′ underwent a decrease when, from Figure 2, the crystalline regions were starting to melt. Again, it is seen the starting point for storage modulus decrease is related to the amount of acidic water used during synthesis with a shift to higher temperature when this was increased.

In the dry PEG network, the silsesquioxane cross-link sites are accumulated in the amorphous regions. The onset of the increase in tan δ represents the α- or glass transition temperature (T_g) in the amorphous region and is related to backbone movement over several repeating units which are confined due to the cross-link points and the crystal domains. These movement limitations cause a shift in the glass transition temperature and change in tan δ peak intensity and shape.[28,31] As shown in Figure 3, the α-transition shifts to higher temperature from sample SW1 to SW4 indicating that the amorphous region is affected by both the cross-link and crystalline region structures.

While the results in SC−DSC and DMTA indicate that the crystalline region structures are affected by the amount of acidic water solution used in the sol−gel reaction, they do not provide details of the chemical structures responsible for these changes. According to Hennink et al.,[11] the number of entanglements can have an effect on the network structures. To better understand whether the changes in the network are controlled by entanglements or the silsesquioxane cross-link structures, ^{29}Si solid state CP/MAS NMR was employed. The silane groups at both ends of PEG in precursor during sol−gel reaction change from T_0 structure (Figure 1 a) into three different structures of Si−O−Si as shown in Figure 4. ^{29}Si solid state CP/MAS NMR is a technique that can

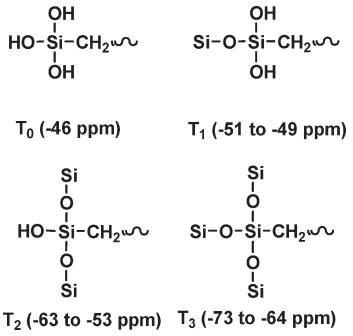

Figure 4. The T structures in organo-hybrid silica are related to the number of O−Si groups (to a maximum of three) that are attached to the organo-silicon atom. The ^{29}Si NMR shifts also are affected by the neighboring groups.

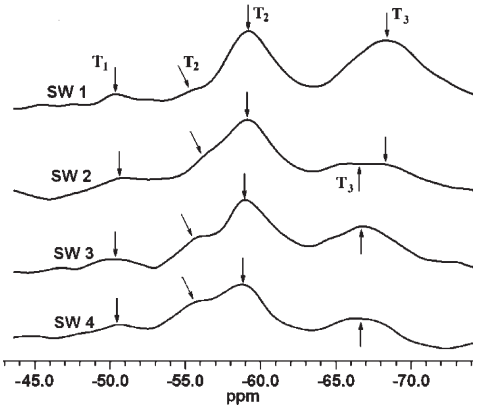

Figure 5. ^{29}Si solid state NMR spectra show the differences between silsesquioxane cross-linker structures (T structures) in networks SW1 to SW4 that were synthesized with a different amount of 0.1 M HCl solution.

distinguish these four different Si−O−Si structures (T_0, T_1, T_2, and T_3) by the chemical shift, as shown.

In Figure 5, ^{29}Si solid state CP/MAS NMR shows different silsesquioxane cross-link structures in PEG networks, depending on the amount of acidic water added. The amount of silicon in the network is very low, and the abundance of ^{29}Si is ~4.67%. These spectra have therefore required acquisition of a large number of transients, which together with the quantitative limitations of cross-polarization, means that quantitative analysis of the spectra is not possible. The shifts in the T structure peaks are caused by the neighboring group changes (Figure 4),[32] which in this case result only from the amount of 0.1 M HCl solution used during synthesis. On increasing the amount of acidic water, the T_3 peak both decreased in intensity and shifted from −68 ppm in SW1 to −66.5 ppm in SW3 and SW4. The higher density of T_3 sites in SW1 implies a larger silsesquioxane domains and consequently a greater number of PEG chains attached. In contrast, in the SW2 network the band is weaker and in fact, two overlapping peaks were seen, implying two slightly different T_3 structures.

The peak in T_2 structures (−63 to −53 ppm) became broader with an increasing amount of acidic water and most interestingly, a small peak at −55 ppm appeared that started as a shoulder on the main peak in SW1 (highlighted in Figure 5) and grew in intensity with higher amounts of added acid. This shoulder may be sensitive to changes in the neighboring groups of T_2 structures that progressively decrease from T_3 (small shoulder in Figure 5) to T_2 or T_1 (intense shoulder in Figure 5) on moving from SW1 to SW4.

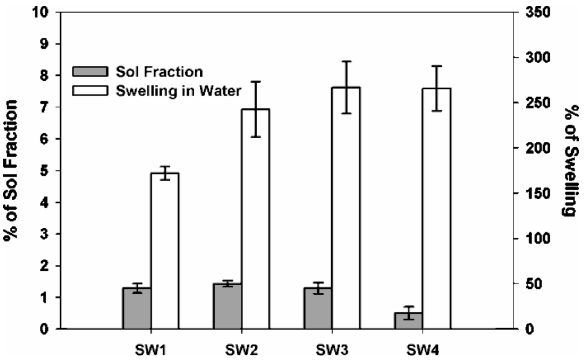

Figure 6. Swelling of hydrogels (synthesized with increased amounts of 0.1 M HCl from SW1 to SW4) when immersed in pure water as well as the sol fractions after extensive extraction.

In summary, the appearance of the broad peak for SW2 in the T_3 region implies two structures are present, i.e., T_3 surrounded by T_2 in addition to other T_3 groups. Support for this is seen in the appearance of the shoulder in the T_2 region from samples SW1 to SW4. This suggests the increased fraction of T_2 units compared to T_3 means that the environment of the T_2 groups is changing to be mostly T_2 instead of T_3. The neighboring group effects on the T structures needs further study by ^{29}Si NMR using isotopically labeled starting materials.

The peak around −51 to −49 ppm represents the T_1 structure, which is quite weak and does not differ greatly in each network. This is most probably an end group in the silsesquioxane structures.[18,33] It may also be seen in Figure 5, in all PEG networks the T_0 peak (−46 ppm) was not seen, which means all silane groups in the precursor have reacted and changed to Si−O−Si linkages. This result is confirmed by the low sol fraction (see Figure 6). This could be due to a lower water solubility of the silane part of precursor (which contains ethoxysilane plus a short linkage chain $-C_3H_6$) compared to the PEG backbone. This may have caused micelle formation through the silane group aggregation when the precursor was dissolved in water. The high concentration of silane in the micelles would assist consumption of the majority of the silane. The different solubility in water between the silane terminus and the PEG backbone that may cause micelle formation has been supported in a related unpublished study by us by changing the [silane/PEG] ratio when the PEG chain length in the precursor was decreased from 2000 to 400 Da. Phase separation was seen in the mixture of PEG 400 precursor and water. Further study, for example by dynamic light scattering, is required to confirm micelle formation.

The structure elucidation by ^{29}Si solid state NMR spectra assists in interpretation of the SC-DSC data on crystallization of the PEG blocks in the networks. The difficulty in cross-link junction movement of the larger silsesquioxane domains during crystallization causes differences in crystalline structures due to constraint on the crystallization process.[34−36] According to Reiter et al.,[37] the constrained crystallization process can be hindered and, as a result, the structures and size of crystal changes. Shibayama et al. showed the crystallization of a polymer network is extensively suppressed in the presence of cross-links.[34,38] Further, Guo et al., show the regularity of crystallites decreases in the restricted PEG chains in the cross-linked network.[39]

In a network with larger silsesquioxane domains (eg SW1) the number of polymer chains attached per cross-link junction is higher than the number in a network with a smaller silsesquioxane domain. The cross-linking junctions in the

PEG network come closer together during crystallization due to chain folding and packing in crystalline regions. When the number of chains that are attached to a silsesquioxane cross-linker is high, such as in the SW1 network, moving the cross-link junctions toward each other is more difficult compared to when the number of attached chains is fewer, such as in SW4. These restricted movements are not the same in the different PEG networks. The PEG crystalline structures showed differences in the crystal transition temperature (Figure 2) and in the α and α′-transition temperatures as measured by DMTA in these networks. This can be seen in the shifts in tan δ where the α-transition temperatures move to higher temperature when the movements become more restricted (Figure 3).

The rate of reactions in hydrolysis and condensation in a sol−gel process depends on the amount of acidic water (both $[H_2O]$ and $[H_3O^+]$). In this study, differences in the rate of reactions were given by the gelation time and led to structure and size differences in the silsesquioxane cross-linkers.[18,26,27] The gelation point in sample SW1 was greatest (more than 1 day) compared to the shortest value of around 2 h for SW4. These differences occur in spite of a decrease in concentration of the other reagent due to an increase in the amount of acidic water added. The shortest gelation time in the SW4 sample produces the smallest silsesquioxane domain, in other words, the number of attached PEG chains is smallest. On the other hand, in the SW1 sample with the longest gelation time, the silsesquioxane domain size is the biggest and the number of attached chains is the highest. Ostwald ripening will be inhibited in these systems due to the bulky PEG groups.

The gelation time effects are consistent with different structures seen in our PEG networks through SC−DSC, DMTA, and ^{29}Si solid state NMR experiments. This is also seen in the properties of the hydrated network (particularly mesh size) through the swelling percentages as discussed in the next section.

Average Molecular Weight between Cross-Links (M_c) and Mesh Size Calculation. Flory et al. found the average molecular weight between two cross-links and polymer network structure (mesh size, ξ) of a cross-linked network may be estimated based on swelling at equilibrium in a specific solvent.[40] This identifies the elastic contribution from deforming the network chains from their initial state, before swelling, up to equilibrium. In this study, both the M_c and mesh size were calculated from swelling of the hydrogels at equilibrium in water.[16] These were calculated using the Flory−Rehner rubber elasticity model:[40,41]

$$\frac{1}{M_c} = \frac{2}{M} - \frac{\frac{v}{V_1}[\ln(1-\nu_{2,s}) + \nu_{2,s} + \chi\nu_{2,s}^{\,2}]}{\left[\nu_{2,s}^{\,1/3} - \frac{\nu_{2,s}}{2}\right]} \qquad (4)$$

where $v_{2,S}$ is the volume fraction of polymer in swollen gel, v is the specific volume fraction of the polymer, χ is the polymer−solvent interaction parameter, V_1 is the molar volume of swelling agent and M is molecular weight of polymer chains before cross-linking. The mesh size (ξ) was calculated from:

$$\xi = \nu_{2,s}^{\,-1/3}\left(\frac{2C_n\overline{M_c}}{M_r}\right)^{1/2} l \qquad (5)$$

where l is the average value of the bond length between C−C and C−O bonds in the repeat unit of PEG (1.46 Å), C_n is the characteristic ratio (C_n = 4.0 for PEG), where M_r is the molecular weight of the repeating unit (44 g/mol).[7]

Table 2. Molecular Weight between Two Cross-Link Junctions (I, Theoretical, and II, Calculated) from Swelling Data[a]

	I		II	
	M_c(theor) (g/mol)	mesh size (theor) (Å)	calculated M_c (g/mol)	mesh size (Å)
SW1	2000	39.8	297	15.4
SW2	2000	43.1	389	18.6
SW3	2000	44.0	439	20.2
SW4	2000	44.0	442	20.4

[a] Mesh size is based on M_c values in hydrogels (synthesized with different amounts of 0.1M HCl) when immersed in pure water.

The results are shown in Figure 6, and the interesting point is the percentage of swelling of hydrogels increased from 172% to 266% only by increasing the amount of acidic water (0.1 M HCl) used in synthesis. The mesh size became bigger from network SW1 to SW4 as shown in Table 2. However, there is a clear disparity between the theoretical value assuming a free chain of PEG with terminal cross-link points (giving M_c of 2000 Da) and the value calculated from the swelling data.

The mesh size was calculated from the measured average molecular weight between cross-links from swelling data (Figure 6) and is found to increase in the PEG silsesquioxane networks from SW1 to SW4 (Table 2). This is consistent with the trends in the crystal transition temperatures of the dry networks and reflects the decrease in size and connectivity of the silsesquioxane domains, as well as the structures which were determined from ^{29}Si solid state CP/MAS NMR.

Although all networks were synthesized from bis(triethoxy silyl propyl urethane)−PEG-2000 (precursor) with the same end-linking method of cross-linking, the average molecular weights between cross-links (M_c) calculated from swelling data are different. During the swelling process in water, the PEG chains that are attached together through the silsesquioxane cross-links are stretched to accommodate more water molecules until they reach the equilibrium chemical potential inside and outside the hydrogels. In this research, the networks are fabricated through end-linking. During swelling and diffusion of solvent into the network the silsesquioxane cross-link sites at each end of PEG chains move away from each other. The conformational entropy of PEG chains is between a maximum in the relaxed state (unconstrained chains) and a minimum in the fully stretched state. The changes in conformational entropy exert forces on the cross-links.[42] In a hydrogel with a bigger silsesquioxane domain (SW1) the number of attached chains is higher, so this force develops faster and reaches a maximum at a lower level of swelling due to constraints to three-dimensional movement of cross-links. The force on the chain and cross-links develops a chemical potential inside the hydrogel network, which increases during the swelling process and when it equals the swelling agent chemical potential outside the hydrogel, the swelling stops. The rate of the force increase in hydrogels is: SW1 > SW2 > SW3 > SW4, however the chemical potential outside the hydrogel is identical for all four hydrogels. The differences in mesh size and M_c between samples SW1 and SW2 are high, compared to the differences between SW3 and SW4. This is because the effects of cross-link structures are not linear on the network properties. Similar nonlinear properties were seen in SC-DSC in Figure 2 and swelling in water in Figure 6.

While the results in Figure 6 can be explained by a thermodynamic argument, the fundamental disparity remains between the theoretical value of M_c and the measured value. This most probably arises from the limitations in the application

of Flory−Rehner theory to a heterogeneous system. The sol fraction (Figure 6) which is an index of un-cross-linked material in the synthesis is only 1.1 ± 0.4% which shows that the majority of the precursor was cross-linked into the network and further, that all hydrogels were stable in water.

Conclusions

A water-swellable network has been synthesized that is cross-linked through silsesquioxane domains formed by hydrolysis and condensation of a bis(triethoxy silyl propyl urethane)−PEG-2000 precursor. The concentration of added acid in the sol−gel reaction controls the kinetics of the cross-linking reaction and thus the network properties without changing the length of the polymer chain. An increase in the amount of acidic water (corresponding to a 3-fold increase in acid concentration from 0.011 to 0.033 mol/L) shifted the dominant silsesquioxane structures from T_3 to T_2 as measured by ^{29}Si solid state CP/MAS NMR. This is consistent with a reduction in the size of the domains when they are formed more rapidly and a decrease in the cross-link density; i.e., there is a reduction in the number of attached chains to each silsesquioxane domain.

It was seen that when the silsesquioxane cross-linker density became higher (i.e., at low concentrations of acid), the relative number of T_3 structures, compared to T_2 structures, increased. The degree of crystallinity by step crystallization−DSC decreased with the increased size of the silsesquioxane domains due to constraints to crystallization by the forces hindering the folding and packing process. Both the glass transition temperature (α-transition) and the screw rotational movement in crystalline regions (α′-transition temperature) showed shifts to lower temperatures with increased size of silsesquioxane domain and a resulting increase in cross-link connectivity. The totally amorphous networks were seen, by the percentage swelling in water, to have a mesh size which also decreased with the size of the sisesquioxane domains, in agreement with the dry network properties.

Acknowledgment. The financial support of the Australian Research Council (Discovery Grant DP 0877988) is gratefully acknowledged. Thanks also go to Dr. Wael Ghafor and Prof. Andrew Whittaker of the AIBN, University of Queensland, for the use of DMTA facilities and Dr. Thor Bostrom and Dr. Christina Theodoropoulos of the AEMF at QUT for TEM analysis.

Supporting Information Available: Figures SI 1−SI 9, showing FT-IR spectra, the bis(triethoxy silyl propyl urethane)−PEG-2000 structure, ^{1}H and ^{13}C NMR spectra, TGA thermograms, photos detailing the different opacities of the networks, and TEM results. This material is available free of charge via the Internet at http://pubs.acs.org.

References and Notes

(1) Wichterle, O.; Lím, D. *Nature* **1960**, *185*, 117–118.
(2) Hoffman, A. S. *Adv. Drug Delivery Rev.* **2002**, *43*, 3–12.
(3) Peppas, N. *Curr. Opin. Colloid Interface Sci.* **1997**, *2*, 531–537.
(4) Alexander, C. *Nat. Mater.* **2008**, *7*, 767–768.
(5) Cruise, G. M.; Hegre, O. D.; Scharp, D. S.; Hubbell, J. A. *Biotechnol Bioeng.* **1998**, *57*, 655–665.
(6) Milton, H. J. *Poly(ethylene glycol) Chemistry: Biotechnical and Biomedical Applications*; Humana Press Inc.: New York, 1992.
(7) Raeber, G.; Lutolf, M.; Hubbell, J. *Biophys. J.* **2005**, *89*, 1374–1388.
(8) Sassi, P.; Blanch, H.; Prausnitz, J. *J. Appl. Polym. Sci.* **1996**, *59*, 1337–1346.
(9) Dai, W.; Barbari, T. *J. Membr. Sci.* **2000**, *171*, 45–58.
(10) Branco, M.; Pochan, D.; Wagner, N.; Schneider, J. *Biomaterials* **2009**, *30*, 1339–1347.
(11) Hennink, W.; Talsma, H.; Borchert, J.; De Smedt, S.; Demeester, J. *J. Controlled Release* **1996**, *39*, 47–55.
(12) Chirila, T. *Biomaterials* **2001**, *22*, 3311–3317.
(13) Badiger, M.; McNeill, M.; Graham, N. *Biomaterials* **1993**, *14*, 1059–1063.
(14) Kweon, J.; Noh, S. *J. Appl. Polym. Sci.* **2003**, *90*, 270–277.
(15) Kweon, J.; Noh, S. *J. Appl. Polym. Sci.* **2001**, *81*, 2471–2479.
(16) Bromberg, L. *J. Appl. Polym. Sci.* **1996**, *59*, 459–466.
(17) Tilgner, I.; Fischer, P.; Bohnen, F.; Rehage, H.; Maier, W. *Microporous Mater.* **1995**, *5*, 77–90.
(18) Brinker, C. J., Scherer, G. W. *Sol-gel Science, the Physics and Chemistry of Sol-gel Processing*; Academic Press: San Diego, CA, 1989.
(19) Nair, B.; Elferink, W.; Keizer, K.; Vereij, H. *J. Colloid Interface Sci.* **1996**, *178*, 565–570.
(20) Van Maris, R.; Tamano, Y.; Yoshimura, H.; Gay, K. M. *J. Cellular Plast.* **2005**, *41*, 305–322.
(21) Muller, A. J.; Arnal, M. L. *Prog. Polym. Sci.* **2005**, *30*, 559–603.
(22) Daniel-da-Silva, A. L.; Bordado, J. C. M.; Martýń-Martýńez, J. M. *J. Appl. Polym. Sci.* **2008**, *107*, 700–709.
(23) Ogoshi, T.; Chujo, Y. *Polymer* **2006**, *47*, 4036–4041.
(24) Aelion, R.; Loebel, A.; Eirich, F. *J. Am. Chem. Soc.* **1950**, *72*, 5705–5712.
(25) Pohl, E. R., Osterholtz, F. D. *Molecular Characterization of Composite Interfaces*; Plenum Press: New York, 1985.
(26) Iler, R. K. *The Chemistry of Silica: Solubility, Polymerization, Colloid and Surface Properties,and Biochemistry*; John Wiley and Sons: New York, 1979.
(27) Voronkov, M. G., Mileshkevich, V. P. Yuzhelevski, Y. A. *The Siloxane Bond*; Consultants Bureau: New York, 1978.
(28) Murayama, T. *Dynamic Mechanical Analysis of Polymeric Material*; Elsevier Scientific Publishing Company: Amsterdam, 1978; Vol. *1*.
(29) Rault, J. *Polym. Rev.* **1997**, *37*, 335–387.
(30) Boyd, R. H. *Polymer* **1985**, *26*, 1123–1133.
(31) Halley, P. J., George, G. A. *Chemorheology of Polymers: From Fundamental Principles to Reactive Processing*; Cambridge University Press: New York, 2009.
(32) Sugahara, Y.; Inoue, T.; Kuroda, K. *J. Mater. Chem.* **1997**, *7*, 53–59.
(33) Pescarmona, P.; Raimondi, M.; Tetteh, J.; McKay, B.; Maschmeyer, T. *J. Phys. Chem. A* **2003**, *107*, 8885–8892.
(34) Qiao, C.; Jiang, S.; Dong, D.; Ji, X.; An, L.; Jiang, B. *Macromol. Rapid Commun.* **2004**, *25*, 659–663.
(35) Takahashi, H.; Shibayama, M.; Hashimoto, M.; Nomura, S. *Macromolecules* **1995**, *28*, 5547–5553.
(36) Hamley, I.; Patrick, J.; Fairclough, A.; Ryan, A.; Bates, F.; Towns-Andrews, E. *Polymer* **1996**, *37*, 4425–4429.
(37) Sommer, J.; Reiter, G. *Phase Transitions: Multinatl. J.* **2004**, *77*, 703–745.
(38) Shibayama, M.; Takahashi, H.; Yamaguchi, H.; Sakurai, S.; Nomura, S. *Polymer* **1994**, *35*, 2944–2951.
(39) Guo, Q.; Slavov, S.; Halley, P. *J. Polym. Sci., Part B: Polym. Phys* **2004**, *42*, 2833–2843.
(40) Flory, P.; Rehner, J. *J. Chem. Phys.* **1943**, *11*, 521–526.
(41) Elbert, D.; Pratt, A.; Lutolf, M.; Halstenberg, S.; Hubbell, J. *J. Controlled Release* **2001**, *76*, 11–25.
(42) Huang, Y.; Szleifer, I.; Peppas, N. *Macromolecules* **2002**, *35*, 1373–1380.